Dennis Wiedemann*, Sylvio Indris[a], Martin Meven, Björn Pedersen, Hans Boysen, Reinhard Uecker, Paul Heitjans and Martin Lerch

Single-crystal neutron diffraction on γ-$LiAlO_2$: structure determination and estimation of lithium diffusion pathway

DOI 10.1515/zkri-2015-1896
Received September 7, 2015; accepted October 26, 2015; published online November 20, 2015

Abstract: γ-Lithium aluminum oxide is a paradigmatic example of an ultraslow lithium ion conductor. This characteristic plays a crucial role in its proposed and actual applications. Herein, we report on the outcome of single-crystal neutron diffraction studies at ambient and high temperature. Careful evaluation confirms the commonly assumed room-temperature structure as derived by powder neutron diffraction in 1965. At 1043 K, a split of the lithium position hints at the onset of intrinsic diffusion. Analysis of the negative scattering-length density using the maximum-entropy method (MEM) indicates a preference for a strongly curved diffusion pathway traversing octahedral voids between adjacent lithium sites. These results help to understand ultraslow lithium diffusion in well-ordered ionic solids on the microscopic scale and, ultimately, to establish structure–property relationships.

[a]Present address: Karlsruher Institut für Technologie, Institut für Angewandte Materialien (IAM-ESS), Hermann-von-Helmholtz-Platz 1, 76344 Eggenstein-Leopoldshafen, Germany
***Corresponding author: Dennis Wiedemann,** Institut für Chemie, Technische Universität Berlin, Straße des 17. Juni 135, 10623 Berlin, Germany, E-mail: dennis.wiedemann@chem.tu-berlin.de
Sylvio Indris and Paul Heitjans: Institut für Physikalische Chemie und Elektrochemie and ZFM – Zentrum für Festkörperchemie und Neue Materialien, Leibniz Universität Hannover, Callinstraße 3–3a, 30167 Hannover, Germany
Martin Meven: Institut für Kristallographie, RWTH Aaachen and Jülich Centre for Neutron Scattering (JCNS) at Heinz Maier-Leibnitz Zentrum (MLZ), Lichtenbergstraße 1, 85747 Garching, Germany
Björn Pedersen: Heinz Maier-Leibnitz Zentrum (MLZ), Technische Universität München, Lichtenbergstraße 1, 85747 Garching, Germany
Hans Boysen: Sektion Kristallographie, Ludwig-Maximilians-Universität München, Theresienstraße 41, 80333 München, Germany
Reinhard Uecker: Leibniz-Institut für Kristallzüchtung, Max-Born-Straße 2, 12489 Berlin, Germany
Martin Lerch: Institut für Chemie, Technische Universität Berlin, Straße des 17. Juni 135, 10623 Berlin, Germany

Keywords: anisotropic displacement parameters; diffusion pathways; high-temperature neutron diffraction; lithium aluminum oxide; maximum-entropy method.

Introduction

Being an ultraslow lithium-ion conductor, γ-$LiAlO_2$ has been discussed for diverse applications: as coating for lithium-conducting electrodes [1, 2], as an additive in composite electrolytes [3], as template for epitaxial growth of III–V semiconductors [4], as membrane material for molten-carbonate fuel cells [5], and as tritium-breeder material in fusion reactors [6, 7]. However, a deeper, microscopic understanding of lithium diffusion in this solid is still lacking.

Although γ-lithium aluminum oxide (γ-lithium aluminate) had been discovered by Weyberg as early as in 1906 [8], it has taken until the emergence of the Rietveld method to unquestionably elucidate its crystal structure using powder X-ray and neutron diffraction in 1965 [9]. In the very same year, single-crystal X-ray diffraction has not only allowed for structure confirmation, but also for the first determination of a crystal's absolute structure [10]. In spite of the interest in more exotic polymorphs of lithium aluminum oxide under ambient and extreme conditions, no further neutron diffraction studies on γ-$LiAlO_2$ have come to our attention.

Constituting a structure type of its own, γ-$LiAlO_2$ crystallizes in the Sohncke groups $P4_12_12$ and $P4_32_12$. It is built of a three dimensional network consisting of pairs of one nearly ideal AlO_4 and one distorted LiO_4 tetrahedron, manifesting itself, *e.g.*, in a highly anisotropic electric field gradient tensor [11]. In these pairs, each corner is shared by two further tetrahedra. Two kinds of channels are formed by octahedral voids in the structure: small ones along the <100> directions and larger ones along [001]. These may play a major role in lithium-ion conduction.

In this study, we present the first single-crystal neutron diffraction experiments on γ-$^7LiAlO_2$ to determine

Bereitgestellt von | Technische Informationsbibliothek Hannover
Angemeldet
Heruntergeladen am | 10.11.17 15:28

its structure at room temperature as well as a high-temperature experiment hinting at possible lithium diffusion pathways.

Experimental

Single crystals of γ-$^7LiAlO_2$ were prepared as described before [11, 12]. Diffraction experiments were performed at FRM II (MLZ, Garching b. München, Germany). Table 1 lists the experimental details. Further details of the crystal structure investigations may be obtained from FIZ Karlsruhe, 76344 Eggenstein-Leopoldshafen, Germany (fax: +49 7247 808-666; e-mail: crysdata@fiz-karlsruhe.de), on quoting the deposition numbers in Table 1.

At 298(2) K, data of a crystal mounted on a glass capillary were collected in κ geometry (ω scans) using the thermal neutron single-crystal diffractometer RESI [16] with Cu(442)-monochromated radiation. Data reduction was performed using EVAL-14 [17]. An analytical absorption correction was performed using the implementation in PLATON [18]. The structure was solved with SHELXS-2014 [19] using direct methods and refined with JANA2006 [20] against F_o^2 data using the full-matrix least-squares algorithm. All ions were refined anisotropically. After final inspection of the F_o vs. F_c plot, four outliers with $|F_o - F_c| > 5\sigma(F_o)$ have been excluded from refinement.

At 1043(5) K (heated with mirror furnace), data of a crystal mounted on a niobium pin in a Eulerian cradle (ϕ/χ scans) with ceramic adhesive were collected using the single-crystal diffractometer on hot source HEiDi [21] with Cu(420)-monochromated ($2\theta_M = 40°$) neutron radiation. The structure was solved with SHELXS-2014 [19] using direct methods and refined with JANA2006 [20] against F_o^2 data using the full-matrix least-squares algorithm. All ions were refined anisotropically. Neither absorption nor extinction correction were necessary (a trial refinement including a Becker–Coppens type 1 parameter for isotropic extinction neither yielded a significant value with $g_{iso} > 3\sigma[g_{iso}]$ nor a justifying model improvement). However, heavy limitations had to be imposed to stabilize the refinement: 19 reflections with $|I - \bar{I}| > 20\sigma(\bar{I})$ have been culled prior to refinement; 26 reflections with $(\sin\theta)/\lambda > 7\ nm^{-1}$, 77 unobserved reflections, and 19 outliers with $|F_o - F_c| > 10\sigma(F_o)$ were excluded.

Maximum-entropy method (MEM) analysis of the scattering-length density was conducted with the program DYSNOMIA 0.9 [22] using 162 structure factors in the zeroth order single-pixel approximation (ZSPA). The unit cell was divided into $160 \times 160 \times 196$ voxels, input uncertainties were adjusted with $E = 0.5$. Because of the low data count, only two generalized constraints C_2 and C_4 with equal weights were employed. Graphics were produced using DIAMOND 3.2 [23] and VESTA 3.3 [24].

Tab. 1: Details of neutron diffractometry on γ-$^7LiAlO_2$.

T/K	298(2)	1043(5)
CSD No.	430184	430185
λ/pm	104.91	55.2
Crystal system	Tetragonal	Tetragonal
Space group	$P4_12_12$	$P4_12_12$
Crystal size/mm³	$3.00 \times 1.64 \times 1.50$	$2.90 \times 2.00 \times 1.90$
a/pm	516.85(4)	525(1)
c/pm	625.65(8)	634(1)
$V/10^6$ pm³	167.13(3)	174.8(7)
ρ_{calc}/g cm^{-3}	2.6198	2.5057
μ/mm^{-1}	0.002	0.002
$2\theta_{max}$/°	99.64	69.62
h_{min}, h_{max}	−4, 6	−4, 10
k_{min}, k_{max}	−6, 4	−6, 10
l_{min}, l_{max}	−8, 6	−12, 13
Absorption correction	Analytical [13]	None
T_{min}, T_{max}	0.9952, 0.9970	–
Extinction correction	B–C type 1 [14, 15]	None
g_{iso}	0.0080(8)	–
Measured reflections	513	1035
Independent reflections (R_{int})	236 (0.1063)	586 (0.1963)
Observed[a] reflections (R_o)	236 (0.0380)	181 (0.1646)
Data, restraints, parameters	232, 0, 21	162, 0, 24
R_1	0.0559	0.0623
wR_2[b]	0.1498	0.1129
u[b]	0.00672	0.00247
S	1.67	1.75
ρ_b(min, max)/ 10^{-6} fm pm^{-3}	0.83, −0.68	0.83, −0.80

[a] $I > 2\sigma(I)$. [b] $w = 1/[\sigma^2(I) + uI^2]$.

Results and discussion

Crystal structures

Because the crystals for diffraction were also used for nuclear magnetic resonance studies, they have been synthesized from isotopically pure lithium-7 reagents [11, 12]. It is safe to assume that isotope effects on the crystal structure – caused by substitution of the 7.59(4)% of naturally abounding lithium-6 [25] – are negligible. However, the difference between the two isotopic compositions had to be considered in neutron diffractometry: the assumed bound coherent scattering length was $b_c = -2.22$ fm (pure lithium-7) instead of $b_c = -1.90$ fm (natural mixture) [26].

Because of the absence of anomalous scatterers in γ-$^7LiAlO_2$, space group $P4_12_12$ was arbitrarily assigned to the specimens instead of $P4_32_12$.

For the dataset acquired at room temperature, structure solution and refinement proceeded without major problems. Apparent effects of strong extinction were handled adequately by introducing a parameter for isotropic extinction of type 1 (Gaussian distribution) according to the Becker–Coppens (B–C) model [14, 15]. All measured reflections were intense enough to classify as "observed".

Bereitgestellt von | Technische Informationsbibliothek Hannover
Angemeldet
Heruntergeladen am | 10.11.17 15:28

The derived structural model (see Table 2 and Figure 1) is identical to the one published in 1965, but data allowed the refinement of more precise harmonic anisotropic displacement parameters (ADPs) for all ions. The final difference Fourier analysis showed no residual scattering-length density in physically sensible positions. The two mentionable minima (*ca.* 30 pm from Li1) and the only maximum (*ca.* 50 pm from O1) are rather small and due to truncation effects.

Unfortunately, the data set acquired at 1043(5) K severely suffers from a slip of the crystal during measurement due to a problem with the ceramic adhesive. The resulting decentering of some reflections caused, amongst other problems, large uncertainties of the cell parameters and a high R_{int}. In spite of the structure solution having been unproblematic, the slip made drastic exclusions necessary in order to stabilize model refinement (*cf.* Experimental): culling of some mismeasured

Tab. 2: Fractional coordinates, displacement parameters U (in 10^4 pm^2), bond lengths (in pm) and angles (in degrees) for γ-$^7LiAlO_2$.

T/K			298(2)			1043(5)
Li1						
Wyckoff pos., site symm.	4*a*	.. 2		8*b*	1	
x, *y*, *z*	0.8096(8)	0.8096(8)	0	0.785(14)	0.826(13)	0.007(10)
U_{11}, U_{22}, U_{33}	0.017(2)	0.017(2)	0.008(3)	0.05(2)	0.044(19)	0.025(8)
U_{12}, U_{13}, U_{23}	−0.0028(19)	0.0004(15)	−0.0004(15)	−0.01(2)	0.014(10)	0.009(16)
U_{eq}	0.0138(13)			0.040(10)		
Al1						
Wyckoff pos., site symm.	4*a*	.. 2		4*a*	.. 2	
x, *y*, *z*	0.1761(5)	0.1761(5)	0	0.1766(7)	0.1766(7)	0
U_{11}, U_{22}, U_{33}	0.0091(11)	0.0091(11)	0.0039(16)	0.0167(12)	0.0167(12)	0.0175(18)
U_{12}, U_{13}, U_{23}	0.0030(10)	−0.0005(7)	0.0005(7)	−0.001(2)	−0.0032(11)	0.0032(11)
U_{eq}	0.0074(8)			0.0170(8)		
O1						
Wyckoff pos., site symm.	8*b*	1		8*b*	1	
x, *y*, *z*	0.3376(3)	0.2901(3)	0.7726(2)	0.3403(4)	0.2862(5)	0.7759(3)
U_{11}, U_{22}, U_{33}	0.0089(9)	0.0127(9)	0.0057(9)	0.0158(10)	0.0333(15)	0.0185(9)
U_{12}, U_{13}, U_{23}	−0.0026(4)	0.0003(4)	0.0004(5)	−0.0042(9)	0.0000(8)	0.0039(9)
U_{eq}	0.0094(5)			0.0226(7)		
d(Li1–O1)	2 × 193.7(3)	2 × 207.9(5)		192(7)	207(7)	
				203(7)	226(7)	
d(Al1–O1)	2 × 175.2(2)	2 × 176.4(3)		2 × 175.8(5)	2 × 178.4(8)	
∢(O1–Li1–O1)	2 × 110.46(13)	2 × 110.60(16)	82.31(17)	104(3)	108(3)	80(2)
			124.5(2)	116(3)	111(3)	126(4)
∢(O1–Al1–O1)	101.72(15)	2 × 110.57(13)	2 × 111.98(11)	103.0(2)	2 × 110.17(19)	2 × 111.95(17)
	109.84(15)			109.5(2)		

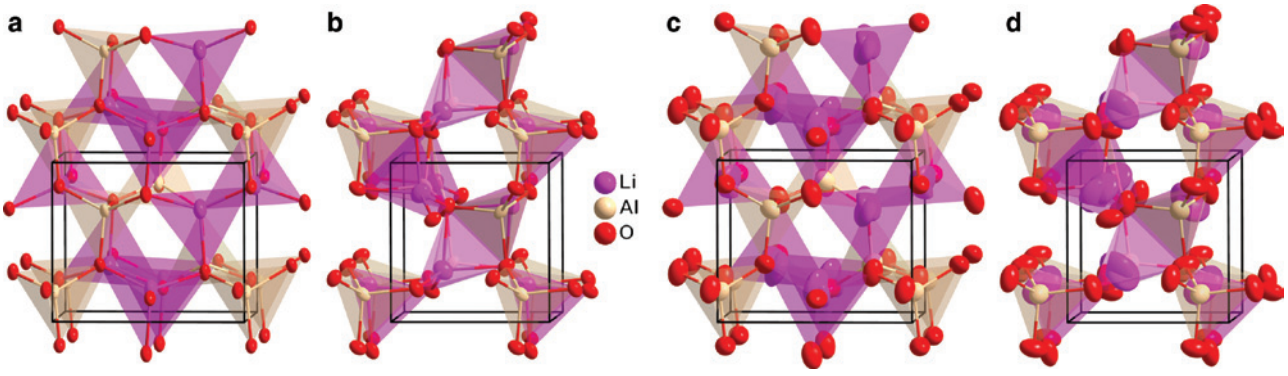

Fig. 1: Crystal structures viewed along *a* (a, c) and along *c* (b, d) at 298(2) K (a, b) and 1043(5) K (c, d). Ellipsoids of 90% probability, unit cell in black, bonds to disordered lithium ions omitted at high temperature for clarity.

Bereitgestellt von | Technische Informationsbibliothek Hannover
Angemeldet
Heruntergeladen am | 10.11.17 15:28

reflections, a cut-off in the high-|***Q***| regime (***Q***: scattering vector), and the exclusion of unobserved reflections (<10% of the count). Several trial refinements were performed using harmonic and anharmonic formulations of the lithium Debye–Waller factor (DWF). Models including only harmonic terms for the lithium ion at the 4*a* site led to a disproportionate growth in ADP parameters for lithium as compared to the other ions. Anharmonic DWF formulations or a split model were able to resolve this issue. All refinements using the former converged to a model having the lithium reference position at (*x*, *x*, 0), as is expected for the structure type, after exclusion of the most insignificant ADPs. Unfortunately, the high-|***Q***| cut-off led to large uncertainties of the anharmonic parameters, rendering them physically meaningless. For this reason, an otherwise inferior split model with the lithium ion at a general 8*b* position – slightly shifted away from the 4*a* site – was found to be the most appropriate (see Table 2 and Figure 1).

With respect to the room-temperature structure, the positional changes for the AlO_2^- framework ions are neglectable; the equivalent ADPs have roughly tripled. The most probable reason for lithium disorder at higher temperature is the onset of thermally activated intrinsic ion diffusion, which has been reported to occur at 1036 K [27].

Lithium diffusion pathways

Diffraction methods provide a time- and space-averaged (over the experiment duration and the whole bulk) picture of the crystal structure. Because of this, dynamic effects reveal themselves as a perceived smearing of scatterer density. The lack of data quality at high temperature unfortunately prohibited a strict analysis of the probability-density function and derivation of the potential landscape. To make best use of the acquired information nonetheless, we have analyzed the scattering-length densities using the MEM. This approach allowes the estimation of a model from a limited amount of information by maximizing information entropy under constraints consistent with observed physical quantities [28]. In the crystallographic case, the MEM gives the maximum variance of calculated structure factors within standard deviations of observed structure factors. Because termination artifacts are less pronounced in comparison with Fourier synthesis (thus resulting in lower noise), the MEM has become a well-established technique in the visualization of lithium diffusion pathways [29, 30].

In the case of γ-$^7LiAlO_2$ at 1043(5) K, the poor data quality made a multiplication of the structure factors' standard uncertainties by *ca.* 1.4 necessary. The MEM reconstruction, being of ample quality ($R_F = 0.0565$, $wR_F = 0.0496$; $C_2 = 1.00$, $C_4 = 0.92$), then converged to a very reasonable scattering-length density distribution reproducing all atom positions and ADP features.

The negative density, to which only the lithium ions contribute, shows a strongly curved path between next-neighboring lithium sites (see Figure 2). This path traverses the octahedral voids, which constitute the channels along [001], but is far from their centers. Above a level of -0.0375×10^{-6} fm pm^{-3}, it is continuously connected, thus signifying a perceivable, but very weak smearing of scattering-length density. Although chunks of density are also visible in the channels along [001], they do not connect above the noise level. This hints at thermally activated self-diffusion being very sluggish at 1043(5) K and only occurring between adjacent lithium sites, not further along channels. However, the latter mechanism may possibly be activated at even higher temperatures.

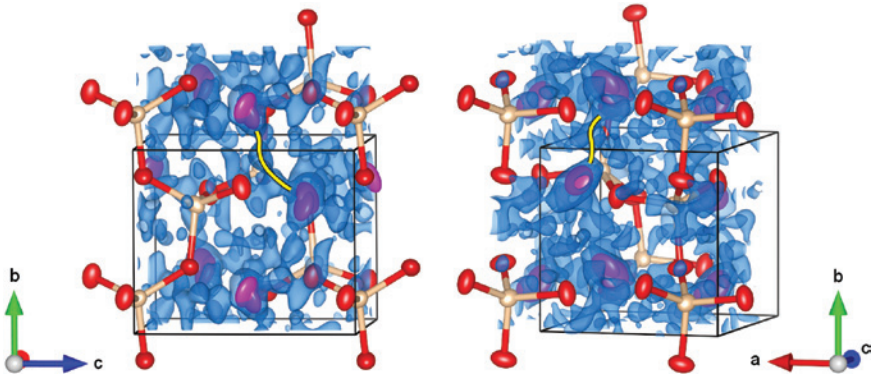

Fig. 2: MEM-reconstructed negative scattering-length density at 1043(5) K in two orientations; pink: lithium ions, ocher: aluminum ions, red: oxide ions (ellipsoids of 75% probability), blue: isosurface for -0.0375×10^{-6} fm pm^{-3}, yellow: proposed lithium diffusion pathway, black: unit cell.

Bereitgestellt von | Technische Informationsbibliothek Hannover
Angemeldet
Heruntergeladen am | 10.11.17 15:28

Conclusion

Our evaluation of single-crystal neutron diffraction data confirms the room-temperature crystal structure (comprising the AlO_2^- framework and the Li^+ position) assigned to γ-$LiAlO_2$ in 1965 and provides more precise data including ADPs. Results of the high-temperature experiment hint at an onset of lithium-ion diffusion around 1043(5) K. The preferred pathway is strongly curved and connects two adjacent lithium positions. Longer-range migration through structural void channels may be possible at even higher temperatures.

Acknowledgments: Financial support by the Deutsche Forschungsgemeinschaft (FOR 1277: "Mobilität von Lithiumionen in Festkörpern [molife]") is gratefully acknowledged. This work is based on experiments performed at the RESI instrument operated by FRM II and the HEiDi instrument operated by RWTH Aachen and Forschungszentrum Jülich within the JARA-FIT initiative at the Forschungs-Neutronenquelle Heinz Maier-Leibnitz (FRM II), Garching, Germany.

References

[1] H. Cao, B. Xia, Y. Zhang, N. Xu, $LiAlO_2$-coated $LiCoO_2$ as cathode material for lithium ion batteries. *Solid State Ionics* **2005**, *176*, 911.

[2] L. Li, Z. Chen, Q. Zhang, M. Xu, X. Zhou, H. Zhu, K. Zhang, A hydrolysis-hydrothermal route for the synthesis of ultrathin $LiAlO_2$-inlaid $LiNi_{0.5}Co_{0.2}Mn_{0.3}O_2$ as a high-performance cathode material for lithium ion batteries. *J. Mater. Chem. A* **2015**, *3*, 894.

[3] M. A. K. L. Dissanayake, Nano-composite solid polymer electrolytes for solid state ionic devices. *Ionics* **2004**, *10*, 221.

[4] P. Waltereit, O. Brandt, A. Trampert, H. T. Grahn, J. Menniger, M. Ramsteiner, M. Reiche, K. H. Ploog, Nitride semiconductors free of electrostatic fields for efficient white light-emitting diodes. *Nature* **2000**, *406*, 865.

[5] H. Takahashi, N. Yamazaki, T. Watanabe, K. Suzuki (Nippon Chemicals Industrial Co.): Gamma Lithium Aluminate Product and Process of Making. US-6,290,928, **2001**.

[6] B. Rasneur, Tritium breeding material: γ-$LiAlO_2$. *Fusion Technol.* **1985**, *8*, 1909.

[7] M. Übeyli, Impact of solid breeder materials on tritium breeding in a hybrid reactor. *J. Fusion Energy* **2006**, *25*, 99.

[8] Z. Weyberg, Ueber einige spinellartige Verbindungen. *Centralbl. Mineral., Geol. Paläontol.* **1906**, 645.

[9] E. F. Bertaut, A. Delapalme, G. Bassi, A. Durif-Varambon, J.-C. Joubert, Structure de γ-$LiAlO_2$. *Bull. Soc. Fr. Minéral. Cristallogr.* **1965**, *88*, 103.

[10] M. Marezio, The crystal structure and anomalous dispersion of γ-$LiAlO_2$. *Acta Crystallogr.* **1965**, *19*, 396.

[11] S. Indris, P. Heitjans, R. Uecker, T. Bredow, Local electronic structure in a $LiAlO_2$ single crystal studied with ^7Li NMR spectroscopy and comparison with quantum chemical calculations. *Phys. Rev. B: Condens. Matter Mater. Phys.* **2006**, *74*, 245120.

[12] S. Indris, P. Heitjans, R. Uecker, B. Roling, Li ion dynamics in a $LiAlO_2$ single crystal studied by ^7Li NMR spectroscopy and conductivity measurements. *J. Phys. Chem. C* **2012**, *116*, 14243.

[13] J. de Meulenaer, H. Tompa, The absorption correction in crystal structure analysis. *Acta Crystallogr.* **1965**, *19*, 1014.

[14] P. J. Becker, P. Coppens, Extinction within the limit of validity of the darwin transfer equations. I. General formalism for primary and secondary extinction and their applications to spherical crystals. *Acta Crystallogr., Sect. A: Cryst. Phys., Diffr., Theor. Gen. Crystallogr.* **1974**, *30*, 129.

[15] P. J. Becker, P. Coppens, Extinction within the limit of validity of the darwin transfer equations. II. Refinement of extinction in spherical crystals of SrF_2 and LiF. *Acta Crystallogr., Sect. A: Cryst. Phys., Diffr., Theor. Gen. Crystallogr.* **1974**, *30*, 148.

[16] B. Pedersen, RESI: Thermal neutron single crystal diffractometer. *J. Large-Scale Res. Facil.* **2015**, *1*, A4.

[17] A. J. M. Duisenberg, L. M. J. Kroon-Batenburg, A. M. M. Schreurs, An intensity evaluation method: EVAL-14. *J. Appl. Crystallogr.* **2003**, *36*, 220.

[18] A. L. Spek, Structure validation in chemical crystallography. *Acta Crystallogr., Sect. D: Biol. Crystallogr.* **2009**, *65*, 148.

[19] G. M. Sheldrick, A short history of SHELX. *Acta Crystallogr., Sect. A: Found. Crystallogr.* **2008**, *64*, 112.

[20] V. Petříček, M. Dušek, L. Palatinus, Crystallographic computing system JANA2006: general features. *Z. Kristallogr. – Cryst. Mater.* **2014**, *229*, 345.

[21] M. Meven, A. Sazonov, HEiDi: single crystal diffractometer at hot source. *J. Large-Scale Res. Facil.* **2015**, *1*, A7.

[22] K. Momma, T. Ikeda, A. A. Belik, F. Izumi, Dysnomia, a computer program for maximum-entropy method (MEM) analysis and its performance in the MEM-based pattern fitting. *Powder Diffr.* **2013**, *28*, 184.

[23] K. Brandenburg, H. Putz, *Diamond 3.2 – Crystal and Molecular Structure Visualization*, Crystal Impact, Bonn (Germany) **2014**.

[24] K. Momma, F. Izumi, *VESTA 3* for three-dimensional visualization of crystal, volumetric and morphology data. *J. Appl. Crystallogr.* **2011**, *44*, 1272.

[25] M. Berglund, M. E. Wieser, Isotopic compositions of the elements 2009 (IUPAC Technical Report). *Pure Appl. Chem.* **2011**, *83*, 397.

[26] V. F. Sears, Scattering lengths for neutrons, in *International Tables for Crystallography*, Vol. C, 3rd ed. (Ed. E. Prince), Kluwer Academic Publishers, Dordrecht (Netherlands) pp. 444, **2004**.

[27] S. Konishi, H. Ohno, Electrical conductivity of polycrystalline Li_2SiO_3 and γ-$LiAlO_2$. *J. Am. Ceram. Soc.* **1984**, *67*, 418.

[28] F. Izumi, Beyond the ability of Rietveld analysis: MEM-based pattern fitting. *Solid State Ionics* **2004**, *172*, 1.

[29] A. Senyshyn, H. Boysen, R. Niewa, J. Banys, M. Kinka, Y. Burak, V. Adamiv, F. Izumi, I. Chumak, H. Fuess, High-temperature properties of lithium tetraborate $Li_2B_4O_7$. *J. Phys. D: Appl. Phys.* **2012**, *45*, 175305.

[30] M. Yashima, Diffusion pathway of mobile ions and crystal structure of ionic and mixed conductors – a brief review. *J. Ceram. Soc. Jpn.* **2009**, *117*, 1055.

Bereitgestellt von | Technische Informationsbibliothek Hannover
Angemeldet
Heruntergeladen am | 10.11.17 15:28